

The multi scenarios applicability of GNSS differential positioning technology in the remeasurement of observatory azimuth in China

Yufei He^{1,2}, Xudong Zhao^{1,2}, Suqin Zhang¹, Qi Li¹, Fuxi Yang³, Shaopeng He⁴, Pengkun Guo⁴ and Jinping Zhou¹

¹Institute of Geophysics, China Earthquake Administration, Beijing, 100081, China

²Beijing Baijiatuan Earth Sciences National Observation and Research Station, Beijing 100095, China

³Xinjiang Earthquake Administration, Urumqi, 830011, China

⁴Hebei Earthquake Administration, Shijiazhuang, 230071, China

Correspondence to: Xudong Zhao (zxd9801@163.com)

Abstract. The azimuth angle of geomagnetic observatory marks is crucial for ensuring the reliability of geomagnetic observation data, and its remeasurement constitutes a core task in observatory operations. The Geomagnetic Network of China comprises 46 geomagnetic observatories, most of which have been in operation for over ten years since their establishment. Thus, completing the azimuth remeasurement at these observatories has become an important mission. By comparing the precision, efficiency, and environmental adaptability of astronomical observation methods and GNSS differential positioning techniques for azimuth measurement, it is found that GNSS differential positioning technology is more suitable for the implementation of this task than traditional astronomical methods. After systematically investigating the multi scenarios in azimuth remeasurement at geomagnetic observatories based on GNSS differential positioning technology, the measurement schemes for five remeasurement scenarios are proposed, which can be applied to measurements under practical conditions such as unobstructed paths, restricted pathways, and single point deployments. Through field validations at the Hongshan, Quanzhou, and Yulin observatories, the feasibility of Scenario I (flat and clear line of sight) and Scenario II (alternative clear path available) is confirmed. Furthermore, a preliminary analysis was conducted on potential error sources in different scenarios, and a prioritized implementation sequence was established for stations that simultaneously meet the conditions of each retest scenario. This work provides a scalable technical solution for azimuth measurement in complex geomagnetic observatories environments.

1 Intruduction

The geomagnetic field, as a fundamental physical field of Earth, not only protects biological evolution but also serves as a key parameter in geoscientific exploration. Geomagnetic observatories, designed for long term continuous monitoring of geomagnetic variations (Jankowski and Sucksdorff, 1996), acquire seven components vector data—total intensity (F), horizontal component (H), declination (D), inclination (I), and Cartesian coordinates (X, Y and Z). These data are extensively

applied in deep resource exploration, high precision navigation, and space environment monitoring (Lu et al., 2022; Lin et al., 2023; Zhang et al., 2024a). Ensuring the precision and accuracy of absolute geomagnetic observations is of paramount importance (Zhang et al., 2024b).

35 It is essential to emphasize that the absolute measurement of the seven geomagnetic components at observatories is achieved through a collaborative system comprising relative recorders and absolute observation devices (St-Louis et al., 2024; Bracke et al., 2025). The relative recorders enable continuous monitoring with a sub second sampling rate, while the absolute observations calibrate baseline values periodically via manual or automated methods (currently focusing on D, I and F components twice weekly). The integration of both systems produces continuous absolute observation data with minute level
40 temporal resolution and accuracy better than 1 nT (Zhang et al., 2016). Consequently, the frequency and precision of absolute observations directly determine baseline reliability, which in turn impacts the quality of final data—this represents the key technical bottleneck in enhancing the accuracy of absolute geomagnetic observations within the current monitoring framework. The magnetic declination (D), defined as the angle between the true north and geomagnetic meridian, is particularly critical for practical applications such as oil drilling and navigation (Shi et al., 2008; Li et al., 2023). Currently, the measurement of
45 magnetic declination (D) at geomagnetic observatories is primarily conducted using fluxgate theodolites instruments (abbreviated as DI instruments), in conjunction with the azimuth angle of the observatory's reference marks. Consequently, the accuracy of the azimuth angle is fundamentally vital to the reliability of these measurements.

The azimuth mark is one of the critical core facilities at geomagnetic observatories, and the azimuth angle, defined as the angle between the true north and line connecting the center of the observation pillar to the center of the mark, is also a vital parameter.
50 Typically, the construction of azimuth marks requires long term stability (CEA, 2004). When feasible, the marks should ideally be engraved or built directly onto bedrock. The measurement of the azimuth angle is generally completed during the observatory's construction phase (Zhou et al., 1997; Xu et al., 2003; Yang et al., 2008; Wang et al., 2014). If the absolute observation chamber of the observatory has not yet been roofed, the azimuth angle can be directly measured at the center of the observation pillar using either astronomical observation methods (Ma, 1995; Cheng et al., 1996; Liu et al., 2020;
55 Khazadryan and Mazurkevich, 2021) or GNSS differential positioning technology (Yin et al., 2008; Zhou et al., 2009; Li et al., 2015; Yu et al., 2018). The azimuth mark and angle are put into service simultaneously with the commencement of the observatory's operations.

The construction of azimuth marks requires long term stability. However, over extended periods of operation at geomagnetic observatories, these marks may undergo displacement due to natural environmental changes or human induced disturbances.
60 For instance, geological tectonic activities (e.g., earthquakes), crustal deformation, or subsurface fluid movements could shift observation pillars. Similarly, urban expansion—such as the construction of large scale facilities nearby, urban loading, or groundwater extraction—may lead to tectonic deformation, causing positional changes in the azimuth marks. Therefore, periodic remeasurements of the mark azimuth angles are essential in geomagnetic observatory operations to verify accuracy and promptly correct errors, thereby ensuring the reliability and precision of geomagnetic data. Azimuth angle remeasurement
65 is a core procedure for maintaining data quality. Consequently, the operating guidelines of China geomagnetic observatory

explicitly require the azimuth angle to be remeasured every 10 years, and if significant changes in the marks are detected, additional assessments need to be conducted immediately (CEA, 2001). The Geomagnetic Network of China consists of 46 geomagnetic observatories, most of which have been in operation for over a decade since their establishment. Thus, completing azimuth remeasurement at these observatories has become an important task.

70 The study first provides a concise introduction to two methods for measuring mark azimuth angles, followed by a comparative analysis. It further examines multi scenarios applicability across diverse geomagnetic observatory environments and proposes five remeasurement schemes based on GNSS differential positioning technology. Field validations at multiple observatories demonstrate the frameworks' effectiveness, offering methodological references for azimuth remeasurement protocols.

2 Azimuth measurement methods

75 Currently, geomagnetic observatories in China mainly use two methods for azimuth measurement: the traditional astronomical observation method and the modern GNSS technology. Both methods can achieve high-precision measurement results.

2.1 Traditional astronomical observation method

The astronomical observation method is a measurement technique that determines the astronomical longitude, latitude, and azimuth of a ground point by observing the positions of celestial bodies (such as the Sun, Polaris, or other stars) and utilizing the relationship between their motion and the Earth's rotation. For traditional astronomical measurements, they are classified into 1 to 4 grades based on measurement accuracy, with the corresponding measurement accuracies being 0.5'' , 1.0'' , 5.0'' , and 10.0'' respectively. In practical measurements, there are also various astronomical observation methods, including the Polaris hour angle method (suitable for grade 1-4 measurements), the solar hour angle method (for grade 4), the multi-star meridian hour angle method (for grade 3-4), the Zinger method (for grade 1-4), the solar altitude method (for grade 4), the multi-star altitude method (grade 1-4), and so on. The celestial bodies to be observed and the observation methods are selected according to the requirements of the measurement grade.

In the northern hemisphere, especially for China, which is located in the mid-low latitudes, Polaris has a declination close to 90 ° and is a brightness star, making it easy to observe. Therefore, the Polaris arbitrary hour angle method is often used to measure the astronomical azimuth. However, since Polaris is not exactly at the North Pole, the precise astronomical longitude and latitude of the observation must be known before measuring the astronomical azimuth (Liu et al., 2020). A brief introduction to the Polaris hour angle method is provided in Appendix A.

2.2 Modern geodetic technology

Modern geodetic technologies for azimuth are primarily implemented via the Global Navigation Satellite System (GNSS), which encompasses satellite positioning systems such as the United States' GPS, Russia's GLONASS, Europe's Galileo, and China's BDS. Typically, GNSS employs two fundamental positioning methods: absolute positioning and relative positioning.

The absolute method provides coordinates with lower precision, so it is used for navigation purposes; in contrast, the relative method delivers coordinates with higher precision and is therefore applied in positioning scenarios. Consequently, the GNSS differential positioning method is commonly utilized in azimuth measurement. The GNSS differential positioning method employs two stationary receivers (one serving as a base station and the other as a rover) to conduct synchronized prolonged continuous observations. Through post processing error elimination and baseline resolution, this technique acquires high precision three dimensional coordinates for both measurement points (A and B). Then transforming coordinates of A and B into a common planar coordinate system (e.g., UTM or local independent coordinate system) following IGS standards. Finally, the azimuth angle is derived from the planar coordinates of reference point (A) and target point (B), using the arctangent function:

$$A = \tan^{-1} \left(\frac{E_B - E_A}{N_B - N_A} \right) \quad (1)$$

where E and N represent easting and northing coordinate differences respectively. This method is not only fast and convenient, enabling near real time acquisition of results, but also unaffected by weather conditions, achieving weather independent operation with all weathers capability, thus exhibiting enhanced operational efficiency. Furthermore, the precision of results can be further improved by appropriately extending the observation time.

Among Modern geodetic methods, it is worth mentioning a calculation method for the azimuth remeasurement based on GNSS networks. By relying on the existing GNSS observation network, this method enables azimuth measurement using only a single GNSS receiver (Sugar et al., 2012). In addition, the widespread use of electronic theodolites has also brought great convenience to azimuth observation. An automatic measurement system composed of an electronic theodolite, a GPS receiver, and a laptop with software for processing measurement data can achieve astronomical measurements that meet Grade 1-2 accuracy requirements (Zhao et al., 2003; Zhang et al., 2005; Solarić and Špoljarić, 1992; Špoljarić and Solarić, 2010).

2.3 Comparison and Selection

A brief comparison between the traditional astronomical observation methods and Modern geodetic technologies is presented in Table 1. Both the methods can achieve high-precision observations, yet each has its own applicable environments. Traditional astronomical observation methods have low reliance on electronic devices and are not affected by electronic signals. However, they are highly dependent on weather conditions, requiring clear skies and good visibility. In contrast, most Modern geodetic technologies rely on GNSS equipment and electronic theodolites. They are easy to operate and can work around the clock, but their performance is poor in environments with insufficient signal coverage or obstructions, and they may be affected by the multipath effect (e.g., increased errors near water surfaces, glass curtain walls, and metal reflective surfaces). According to actual observation data, the maximum GPS positioning error caused by the multipath effect can reach 3.4 cm (Fu, 2004). In high-reflection environments, this error can be as large as 15 cm (Wang, 2000). When the distance from a high-reflection surface is approximately 50 meters or more, the multipath effect can basically be neglected (He, 2010). The two methods are

irreplaceable to each other, complementing one another in terms of precision and environmental adaptability. In practical work, measurement methods can be flexibly selected according to the application scenarios.

130 **Table 1: Comparison of Azimuth Measurement Methods**

Method	Traditional Astronomical Observation	Modern Geodetic Technology
Equipment	Theodolite, ephemeris, timer	GNSS receivers, electronic theodolites , data processing software
Limitations	Requires clear skies or visible celestial body	Requires open sky, susceptible to obstructions
Complexity	High (astronomy expertise needed)	Low (automated)
Precision	0.5" (Polaris based first class measurement)	1"~2" (ideal conditions)
Applications	Remote areas, military operations, heritage restoration	Engineering survey, UAV navigation, traffic planning
Error Sources	Atmospheric refraction, timing errors, instrument alignment	Multipath effects, ionospheric delay, satellite geometry
Cost	Economical	Expensive

The Geomagnetic Network of China comprises 46 geomagnetic observatories, most of which have been in operation for over 10 years, and their azimuth angles all require re-measurement. The mark’s azimuths of the early-constructed observatories were measured using traditional astronomical methods, and usually obtained during the station construction period. At that
135 time, the observation rooms were not yet roofed, and theodolites could be set up directly on observation pillars to achieve unobstructed visibility of Polaris. Today, however, the rooms have been fully roofed, making it impossible to see the sky from inside. Moreover, the fixed mark pillars outdoors vary in shape (as shown in Fig.1), and are mostly unsuitable for mounting theodolites on them. Furthermore, traditional astronomical observation is highly dependent on weather conditions. Due to the diverse geographical locations of the observatories, especially those in coastal areas, where cloudy weather is frequent. It
140 sometimes often takes several days of waiting for suitable weather to conduct astronomical method, making the measurement process time consuming and inconvenient for arranging remeasurement plans.

In traditional astronomical observation methods, the Sun can be used as the observed celestial body to measure azimuth, but it can only achieve a relatively low level of accuracy (about 10"), as stated in the IAGA guidelines (Newitt et al., 1996). Although Solarić et al. (1988, 1990) achieved high accuracy based on a large amount of solar observation data, and pointed
145 out that the accuracy is particularly better during sunrise and sunset periods. For high-precision observations, especially for achieving Grade 1-2 astronomical observations, and considering the current conditions of the observatories, the solar based azimuth observation method is not suitable for the re-measurement work of the 46 observatories in the network. Therefore, after considering factors such as measurement scenarios, time cost, and operational convenience, the GNSS differential positioning method was selected to complete the remeasurement work.



Figure 1: Different styles of azimuth marks

3 Multi scenarios analysis for azimuth remeasurement

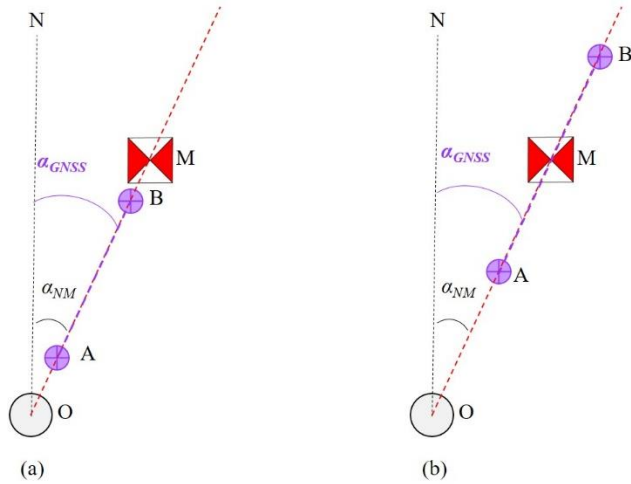
In measurements based on GNSS differential positioning method, due to the varying observational conditions (such as line of sight conditions, terrain features, and surrounding vegetation coverage) across stations, require tailored measurement approaches for different scenarios. The following section discusses five common situations that may be encountered during such remeasurements.

3.1 Scenario I: Flat and clear line of sight

If the path between the observation pillar in the geomagnetic absolute observation room and the azimuth mark is flat and unobstructed, and free from tall vegetation coverage, two GNSS receivers can be deployed along the line of sight (LOS), with sufficient separation distance (for GNSS receivers with a horizontal positioning error of 2 mm, a minimum distance of 200 m between them is required to achieve 2" level measurement accuracy). Additionally, the targets of both GNSS receivers are visible from the observation pillar. During this remeasurement scenario, the GNSS receivers should be installed along the unobstructed line of sight path while ensuring sufficient distance between them. A high precision theodolite (1" level) must be used to align the azimuth mark and the two GNSS targets, guaranteeing that the center of the observation pillar, the azimuth mark, and both targets lie on a single straight line. The detailed process of installing two GNSS targets on the straight line is provided in Appendix B.

Figure 2 illustrates the schematic diagram for calculating the azimuth angle based on this method, where O represents the center of the observation pillar, A and B denote the two GNSS receiver points, M is the azimuth mark, and a_{NM} and a_{GNSS} indicate the azimuth angles of the azimuth mark and the GNSS receiver line, respectively (these symbols retain the same meaning in subsequent schematic diagrams and will not be reiterated in later sections). If the OM distance is sufficiently long to meet measurement requirements, points A and B can be installed between O and M, as shown in Fig. 2(a). However, if the

distance between A and B is too short to satisfy measurement criteria, point B can be relocated beyond mark M to a farther position, as depicted in Fig. 2(b).



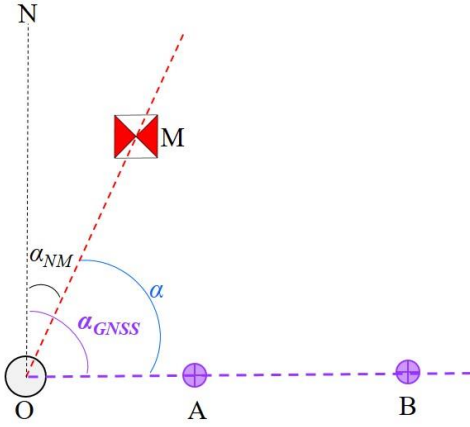
175 **Figure 2: GNSS collinear deployment**

As shown in Fig. 2, since points O, A, B, and M lie on the same straight line, the azimuth angle of the OM connection (α_{NM}) is identical to the azimuth angle of the line connecting the two GNSS receiver points A and B (α_{GNSS}). In this scenario, the azimuth angle of the GNSS receiver line is equivalent to that of the azimuth mark:

$$\alpha_{NM} = \alpha_{GNSS} \quad (2)$$

180 **3.2 Scenario II: Alternative clear path available**

When there is a clear line of sight between the observation pillar and the azimuth mark, but the path is obstructed by tall vegetation (which may interfere with GNSS satellite signal reception), or the terrain along the path is uneven (preventing visual alignment of targets from the pillar), or the path lacks sufficient distance to deploy two GNSS receivers, an alternative survey line in another direction with clear visibility and sufficient length can be identified. In such scenarios, the GNSS receivers can be deployed along this alternative survey line. By conducting GNSS measurements, the azimuth angle of this line can be determined. Subsequently, using a high precision theodolite (1" level) to measure the angle between this line and the azimuth mark's path, the azimuth angle of the mark can ultimately be derived. Figure 3 provides a schematic diagram of this measurement method.



190 **Figure 3: Alternative path GNSS deployment**

As shown in Fig. 3, since points O, A, and B are collinear, the GNSS receivers at A and B can measure the azimuth angle of this line (a_{GNSS}). The angle α between the OM line and the collinear line OB can be determined through repeated measurements with a high precision theodolite (1" level). In this scenarios , the azimuth angle of the observation mark OM (a_{NM}) is derived via the following formula:

195
$$a_{NM} = a_{GNSS} - \alpha \quad (3)$$

3.3 Scenario III: Single GNSS receiver on LOS

When there is clear line of sight between the observation pillar and the azimuth mark, but insufficient distance or obstructions from tall vegetation prevents to deploy two GNSS receivers along this direction, and only one GNSS receiver is feasible. In such scenario, the following approach can be adopted. One GNSS receiver can be deployed along the path between the observation pillar and the azimuth mark. The second GNSS receiver can be placed on another path with clear mutual visibility to the first GNSS receiver, ensuring the distance meets measurement requirements. Then the azimuth angle of the GNSS baseline can be determined using GNSS differential methods. Subsequently, a high precision theodolite, mounted on the tripod at the first GNSS receiver point, can be used to measure the angle between Point O (or Point M, depending on field setup constraints) and the GNSS target at Point B by conducting repeated measurements. The azimuth angle of the mark can be ultimately calculated using the two angles, as illustrated in Fig. 4.

205

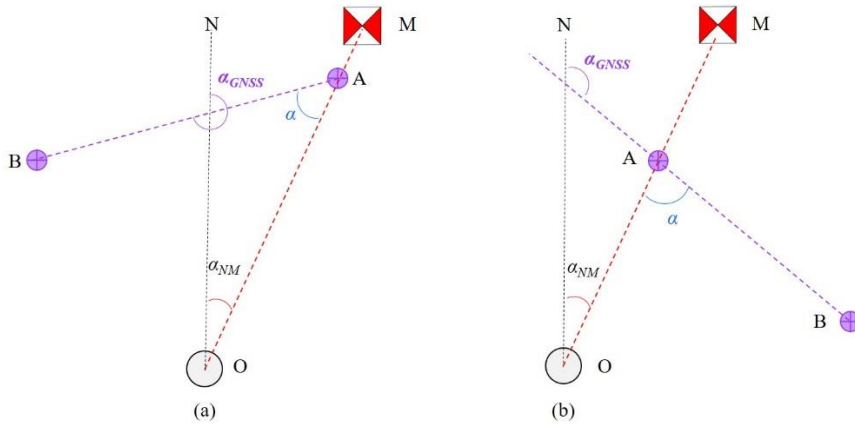


Figure 4: Single GNSS on main path, (a) B is left of A, (b) B is right of A

Figures 4(a) and (b) illustrate the two scenarios where Point B located to the left and right of Point A, respectively. Points O, A, and M are collinear. The azimuth angle of the baseline AB is denoted as α_{GNSS} . The angle between AB and AO is α . The azimuth angle of the mark (α_{NM}) can be calculated as follows:

$$\alpha_{NM} = \begin{cases} \alpha_{GNSS} - 180^\circ - \alpha, & (B \text{ is left of } A) \\ \alpha_{GNSS} - (180^\circ - \alpha), & (B \text{ is right of } A) \end{cases} \quad (4)$$

3.4 Scenario IV: Single GNSS receiver on alternative path

If no suitable locations are available for deploying GNSS receivers along the direct path between the observation pillar and the azimuth mark, but an alternate point can be identified that maintains line of sight with both the observation pillar and another measurement point meeting distance requirements. The following workflow can be applied in this scenario. First, two GNSS receivers can be deployed at the two measurement points. The azimuth angle of the GNSS baseline connecting the two GNSS receivers can be measured using GNSS differential positioning. Subsequently, a high precision theodolite can be mounted at the GNSS receiver point which is visible to the observation pillar. Through repeated measurements, the angular offset between the second GNSS point and the center of the observation pillar is determined. The theodolite is then relocated to the observation pillar, where repeated measurements are conducted to obtain the angular between the azimuth mark and the visible GNSS point. Finally, the azimuth angle of the azimuth mark is calculated based on the angular relationships derived from these measurements. A schematic diagram of the measurement process is illustrated in Fig. 5.

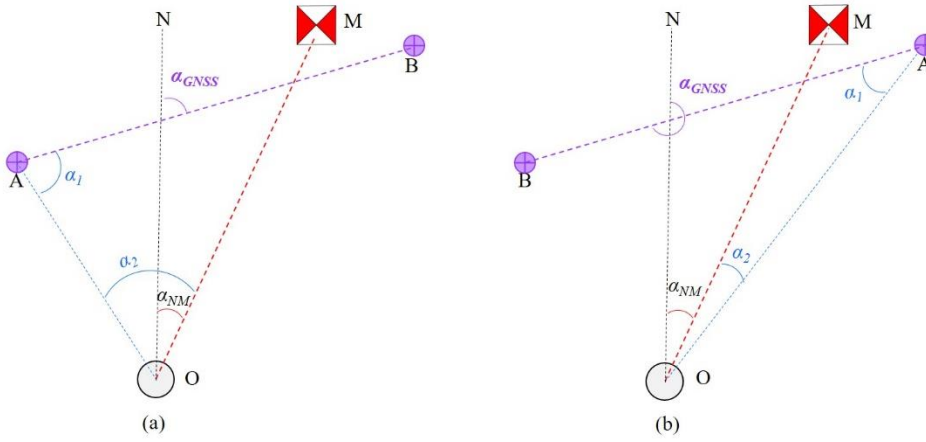


Figure 5. Single point visibility measurement on alternative path, (a) B is right of A, (b) B is left of A

In Fig. 5, Point A is mutually visible to both the center of the observation pillar (O) and measurement point B. Figures 5(a) and (b) depict scenarios where Point B is positioned to the right and left of Point A, respectively. Here, a_{GNSS} denotes the azimuth angle measured by GNSS differential positioning, while α_1 and α_2 represent the angular offsets observed at Point A and the observation pillar. Based on the angular relationships illustrated in the figures, the azimuth angle of the azimuth mark is calculated as follows:

$$a_{NM} = \begin{cases} (a_{GNSS} - 180^\circ) - \alpha_1 - \alpha_2, & (B \text{ is left of } A) \\ a_{GNSS} - (180^\circ - \alpha_1 - \alpha_2), & (B \text{ is right of } A) \end{cases} \quad (5)$$

3.5 Scenario V: No GNSS deployment feasibility

If none of the preceding scenarios are applicable (i.e., no GNSS compatible locations exist within the line of sight range of the observation pillar in the observation room), but an auxiliary point can be identified that is both mutually visible to the observation pillar and aligned with a survey line that meets GNSS deployment requirements. Then the remeasurements can be completed rely on the auxiliary mutually visible point.

Most geomagnetic observatories were equipped with calibration huts containing an observation pillar. This pillar was designed to maintain mutual visibility with the observation pillar in observation room and to offer clear sightlines to its surroundings (if Polaris could be observed from this pillar, astronomical azimuth methods could theoretically be applied, though this is not discussed here). If a specific direction near the pillar provides unobstructed visibility and meets the requirements for deploying two GNSS receivers, the pillar can serve as an auxiliary reference point. If such a pillar is not available at the observatory, a tripod can be set up at the location to act as a temporary auxiliary point.

In this scenario, a high precision theodolite is set up at the auxiliary point (either the observation pillar in the calibration hut or a tripod mounted location). The theodolite is aligned to ensure that the two GNSS measurement points lie on the same survey line. Through repeated measurements, the angular α_1 between the target mark of either GNSS and the center O (marked by a fine needle secured with clay) of the observation pillar in the observation room is determined. Subsequently, the high

precision theodolite is relocated to the observation pillar inside the observation room, where repeated measurements the
 angular a_2 between the azimuth mark and the center P of the auxiliary point. Finally, by integrating the results from GNSS
 250 differential positioning, the azimuth angle of the azimuth mark can be calculated. Figure 6 illustrates a schematic diagram of
 this measurement method.

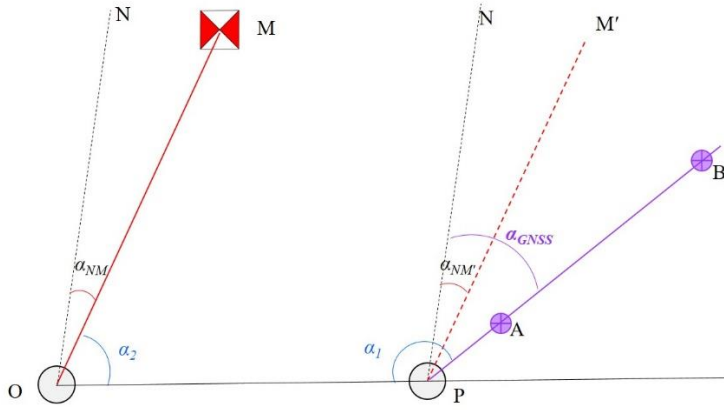


Figure 6. Indirect measurement via auxiliary point.

In Fig. 6, point P represents the center of the auxiliary measurement point (observation pillar or tripod setup), and PM' is the
 255 parallel line to OM . Thus, the azimuth angle a_{NM} equals $a_{NM'}$. From the angular relationships shown in the figure, the azimuth
 angle of the mark can be derived as:

$$a_{NM} = a_{GNSS} - (a_1 + a_2 - 180^\circ) \quad (6)$$

4 Multi scenarios case studies in azimuth remeasurement

The previous text analyzed five potential scenarios for azimuth remeasurement and provided corresponding measurement
 260 solutions. Based on these scenarios, we have preliminarily initiated remeasurements at stations with long standing azimuth
 marks and obtained initial results. Currently, azimuth remeasurements have been completed at three stations: Hongshan
 Geomagnetic Observatory, Quanzhou Geomagnetic Observatory, and Yulin Geomagnetic Observatory.

Hongshan Geomagnetic Observatory, located in the North China Plain, started its previous azimuth mark in 2003 (22 years
 ago); the path between its observation pillar and azimuth mark features flat terrain with a completely unobstructed line of sight,
 265 satisfying Scenario I conditions, hence Scenario I methodology was adopted. Quanzhou Geomagnetic Observatory in
 southeastern China's hilly terrain has its azimuth mark engraved on bedrock, dating back to 2007 (18 years ago); although the
 path is complex, two measurement point meeting Scenario I requirements can be identified, so Scenario I was applied. Yulin
 Geomagnetic Observatory, located in the suburban area of Yulin, northwestern China, had its original primary azimuth mark
 destroyed. However, before its destruction, the azimuth angle was transferred to the rooftop of a distant building and has been
 270 in use since 2009 (16 years ago). Due to multiple buildings and tall trees obstructing the path, measurements using Scenario I

were unfeasible. Fortunately, an alternative survey line meeting Scenario II requirements was identified from the opposite side of the observation room, enabling azimuth remeasurement via Scenario II. Additionally, Scenario IV methodology was also attempted in Yulin observatory. Detailed results for all three observatories are presented in Table 2.

Table 2. Comparison of remeasured and original azimuth angles

Observatory	Scenario	Pillar No.	Remeasured (GNSS)		Original (Astronomy)	Difference
			Azimuth	Standard deviation	Azimuth	
Hongshan	I	1#	1° 31' 55.8"	±2.1"	1° 31' 52.2"	3.6"
		2#	2° 22' 10.8"	±1.6"	2° 22' 9.6"	1.2"
Quanzhou	I	1#	179° 46' 37.9"	±0.7"	179° 46' 28.6"	9.3"
		5#	178° 30' 34.4"	±0.8"	178° 30' 25.6"	8.8"
Yulin	II	1#	354° 49' 40.2"	±0.7"	354° 49' 31.2"	9.0"
	IV	1#	354° 48' 49.3"	±0.7"		41.9"

275

In the azimuth remeasurement work at these three geomagnetic observatories, we uniformly used the GNSS equipment with the rapid static horizontal accuracy 2.5mm+0.5ppm RMS, employed the Zeiss Theo 010B theodolite with an angular measurement accuracy of 1^{cc} (0.324"), war used for collinearity alignment and angle measurement. Additionally, three sets of data were collected for each GNSS survey line (in the WGS84 coordinate system), and the mean value and standard deviation are presented in Table 2. Most of the differences between the re-measured azimuths and the original astronomical azimuths are within the range of 0-9" . However, in the Scenario IV test at Yulin observatory, a significant deviation (41.9") was observed between the measured and original results. **Three primary** factors may contribute to this result. The first one is the insufficient GNSS baseline length. Despite the RMSE of three measurement sets remained stable at 0.7" , the short distance between two GNSS points (about 60 m) and the maximum horizontal error (about 2.5 mm) may introduce the potential angular error of up to 8.6" . The second one is the theodolite setup error. In this scenario, the theodolite needs to be installed on the tripod at point A, as shown in Fig. 5(b). During angle measurement process, a centering offset was detected on the tripod. After re-centering, a change of 10.8" occurred. This underscores the necessity of adequate baseline distances and highlights the need for further analysis of tripod measurement error characteristics. **The last one is that measurement errors will be introduced when measuring the angles between the azimuth mark and the GNSS target in Scenario II and IV using theodolite. In this work, each angle was measured 6 times. The standard deviation of angle α in Fig. 3 of Scenario II is 2.5" , and standard deviation of angle α_1 and α_2 in Fig. 5b of Scenario IV are 3.3" and 1.8" , respectively. It can also be noted that the standard deviation of the angle (α and α_2) measured on the observation pillar is smaller than that (α_1) on the tripod. Therefore, the stability of observation points is also important. Compared with the difference in Table 2, the measurement errors cannot be ignored in**

280

285

290

the analysis. In order to reduce the error introduced by the measured angle, it is necessary to increase the number of repeated measurements.

It should be noted that the azimuth obtained by the astronomical observation method is referenced the plumb line, while the azimuth obtained by the geodetic method (derive from the GNSS method) is based on the ellipsoidal normal. So the vertical deflection introduces systematic error to the azimuths (Vittuari et al., 2016). For example, Šugar et al. (2012) compared azimuths obtained from astronomical methods and GNSS measurements, finding an average difference of $0.8''$, and the standard deviation of the astronomical azimuth was $\pm 2.6''$. Based on 14 astronomical observations and comparative experiments with GNSS, Wang et al. (2001) reported that the differences between the two methods mostly ranged between $0-3''$, with a maximum difference of up to $4.5''$.

Accounting for the influence of vertical deflection, it is necessary to apply the Laplace azimuth equation (7) to convert the astronomical azimuth to the ellipsoidal normal based azimuth (Torge, 2001),

$$a - A = -\eta \tan \varphi + \frac{\eta \cos \alpha - \xi \sin \alpha}{\tan \zeta} \quad (7)$$

where A is the azimuth determined by astronomic observation and referred to the plumb line, a is the azimuth referred to the ellipsoid normal, ζ is the ellipsoidal zenith-distance to the reference mark, η and ξ are the components of the deflection of the vertical: $\xi = \Phi - \varphi$ and $\eta = (\Lambda - \lambda) \cos \varphi$. They can be calculated by the astronomic coordinates (Φ, Λ) and the ellipsoidal coordinates (φ, λ) . Due to the lack of astronomical latitude Φ and longitude Λ values for the measured points, it is temporarily impossible to conduct this calculation. However, the global gravity field model provides a way to calculate the vertical deflection. Based on the gravity field model EGM2008 (<https://icgem.gfz-potsdam.de/>), the vertical deflections at the measurement point were calculated in the WGS84 coordinate system, including the north-south component ξ and the east-west component η . After providing the zenith distance ζ of the azimuth marker, the geodetic azimuth of the azimuth mark can be finally calculated according to formula (7), and then the difference with the GNSS results can be computed, as shown in Table 3. It can be seen that the difference between the converted azimuth and the re measured azimuth has decreased, with the difference generally within $5''$. Therefore, when considering systematic deviations between astronomical and GNSS methods, positioning errors, sighting alignment errors, and other factors, a discrepancy of $0-5''$ is within expected limits. In addition, assuming that the azimuth mark has shifted, for an azimuth mark located 200m from the observation pillar center, it would need to be displaced 5 mm in the direction perpendicular to the line connecting the two to achieve a $5''$ discrepancy (the displacement occurring in the direction of the connection between the two cannot be detected). Furthermore, in terms of the accuracy requirement for azimuth in absolute geomagnetic observation ($0.1'$), a variation of $0-5''$ over several decades is considered acceptable. Thus, it can be concluded that no significant displacement has occurred at the observation marks. The previous measurement results can also serve as reference for results evaluation.

Table 3. The converted azimuth angle after vertical deflection correction and its difference from CNSS results

Observatory	Scenario	Pillar No.	Vertical deflection		Zenith Distance	Corrected Angle	Converted Azimuth	Difference
			η (")	ξ (")	ζ (°)	ΔA (")	a	
Hongshan	I	1#	-1.57120	-2.45921	89.98065	1.20077	1°31'53.4"	2.4"
		2#			89.97359	1.20060	2°22'10.8"	0.0"
Quanzhou	I	1#	-8.49674	3.83258	86.44249	4.48940	179°46'33.1"	4.8"
		5#			86.24792	4.51258	178°30'30.1"	4.3"
Yulin	II	1#	-8.86352	-2.51050	89.96663	7.01978	354°49'38.2"	2.0"
	IV	1#						48.9"

5 Conclusions

This paper proposes five applicable remeasurement scenarios based on GNSS differential positioning, comprehensively covering all remeasurement challenges. Comparative analysis reveals: Scenario I requires only GNSS receiver alignment (ensuring collinear points), simplifying operations without angular measurements or conversions, thus introducing no additional errors beyond four points alignment inaccuracies. Scenarios II and III necessitate measuring one angle (beyond alignment), introducing single error sources. However, Scenario II performs this measurement on more stable observation pillars, while Scenario III uses tripods, making Scenario II superior. Scenarios IV and V require measuring two angles (introducing dual errors), with one typically tripod based. If Scenario V employs a stable observation pillar as an auxiliary point, it outperforms Scenario IV. Consequently, based on the principle of ‘one more measurement, one more error introduced’, in order to minimize the introduction of errors, the priority order of measurement schemes for remeasurement is as follows: Scenario I (optimal) > Scenario II > Scenario III > Scenario V (with fixed pillar) > Scenario IV.

Field measurements at three observatories using Scenarios I and II confirm the feasibility of these remeasurement methods. Remeasurements show minimal azimuthal changes at all three observatories. Quanzhou’s mark is engraved on bedrock; Hongshan’s mark is mounted on a pillar with a stable foundation on level ground; Yulin’s original mark was destroyed, and its mark relocated to a distant rooftop (relatively stable but weather vulnerable and not recommended for permanent marks). These cases highlight that mark stability of azimuth marks is crucial.

A slight change of azimuth mark was detected at these three observatories. Due to the small changes, which is basically within the measurement error range, but still meet the requirements of the magnetic declination accuracy of the geomagnetic observatories, it can be concluded that the azimuth markers at all three stations remained unchanged. However, in future measurements, particularly for angle measurements in scenarios other than Scenario I, increasing the number of measurement repetitions is highly recommended to improve observation accuracy. In any case, these findings enhance the data accuracy assurance for observatory operations and verify the importance of this work.

Appendix A: Polaris hour angle method

Figure A1 illustrates the angular relationships among the azimuth mark, celestial body, and true north in the horizontal coordinate system centered at observation point O . In this system: Z represents the zenith, M denotes the ground azimuth mark, S' is the projection of celestial body S onto the horizontal plane, P stands the north pole, N is the intersection point of the great circle passing through the zenith and the north pole with the horizon. A indicates the celestial body's azimuth angle, and θ signifies the horizontal angle between the celestial body and the mark. To determine the azimuth angle (a_{NM}) of OM, the following two steps are required: (a) measure the horizontal angle θ between the celestial body and the mark; (b) record the observation time and calculate the celestial body's azimuth angle A . Finally, the azimuth angle a_{NM} can be derived as follows:

$$a_{NM} = A + \theta \quad (A1)$$

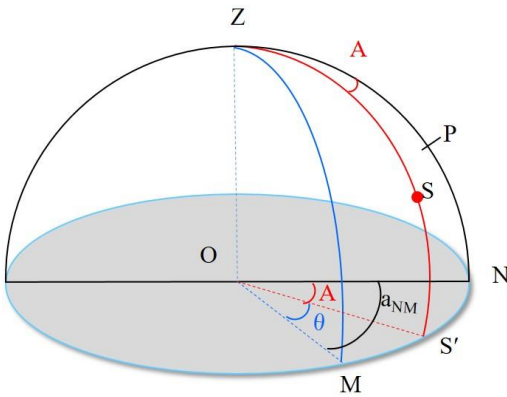


Figure A1: Spherical Diagram of Astronomical Azimuth

Figure A2 shows the spherical triangle ΔZPS used to calculate the azimuth of Polaris. Based on the altitude angle h of Polaris in the horizontal coordinate system, the latitude φ of the observation point, the declination δ of Polaris, and its hour angle t , the formula for calculating the celestial azimuth A (with the positive direction being eastward from north) can be derived using spherical trigonometry:

$$A = \tan^{-1} \left(\frac{-\sin t}{\cos \varphi \tan \delta - \sin \varphi \cos t} \right) \quad (A2)$$

azimuth mark. Figure B1(a) demonstrates azimuth mark alignment: After precisely centering the azimuth mark using the telescope crosshairs, the horizontal circle should be locked in place. Figure B1 (b) shows initial positioning: The tripod with the GNSS target should be aligned with the sightline formed by the telescope crosshairs and the azimuth mark. Figure B1 (c) depicts the first aligned GNSS receiver, while Fig. B1 (d) presents the second aligned GNSS receiver and azimuth mark.



Figure B1: Theodolite alignment to the GNSS targets and the azimuth mark.

Data availability

All raw data can be provided by the corresponding authors upon request.

Author contribution

YH and XZ initiated the study. SZ and QL designed the analysis methods. FY, SH and PG carried them out. JZ provided photos of the azimuth marks. YH prepared the manuscript with contributions from all coauthors.

Competing Interests

The authors have no competing interests to declare.

Acknowledgements

We express our gratitude to the colleagues at Hongshan geomagnetic observatory, Quanzhou geomagnetic observatory, and Yulin geomagnetic observatory for their assistance during the azimuth remeasurement process, which enabled the smooth completion of the survey work.

Funding Information

Supported by National Natural Science Foundation of China (42374092); The Special Fund of the Institute of Geophysics, China Earthquake Administration (Grant Number DQJB25X26); National Key R&D Program of China (2023YFC3007404).

References

- Bracke, S., INTERMAGNET Operations Committee and Executive Council: INTERMAGNET Technical Reference Manual, Version 5.2.0, https://tech-man.intermagnet.org/_/downloads/en/stable/pdf/, Last accessed 20 May 2025.
- 410 Cheng P.G., Li J.P. and Yu X.H.: Software of analytic method for determining astronomical azimuth, *Engineering of Surveying and Mapping*, 5(4):44-50, 1996.
- China Earthquake Administration (CEA): Specification for the construction of seismic station: Geomagnetic station (in Chinese). DB/T 9–2004. Beijing: Seismological Publishing House. 2004.
- China Earthquake Administration (CEA): Technical specifications for digital seismic and precursor observation: Electromagnetic Observation (Trial Implementation) [M]. Beijing: Seismological Publishing House, 11-16, 2001.
- 415 Fu P.Y.: The analysis of multipath error of GPS measuring with practical data, *Chinese Journal of Scientific Instrument*, 25(4): 748-749, 2004.
- He Y.L.: The study of multi-path effects on high precision GPS surveying, *Engineering of Surveying and Mapping*, 19(1): 35-38, 2010.
- 420 Jankowski, J., and Sucksdorff, C.: Absolute magnetic measurement, in: *Guide for magnetic measurements and observatory practice*, IAGA, Warszawa, Poland, 87–102, 1996.
- Newitt, L.R., Barton, C.E., and Bitterly, J. (Eds.): *Guide for Magnetic Repeat Station Surveys*, IAGA, USA, 37-38 pp., ISBN: 0-9650686-1-7, 1996,
- Khanzadyan M. A. and Mazurkevich A.V.: Development of a method for measuring the astronomical azimuth using an electronic total station. *E3S Web of Conferences*, 310(03007), <https://doi.org/10.1051/e3sconf/202131003007>, 2021.
- 425 Li S.M., Wang G.G. and Shen Z.F.: Theory, method and application of positioning and navigation of geomagnetic field, *Gnss World of China*, 2023, 48(6): 42-51. DOI: 10.12265/j.gnss.2023141, 2023.
- Li Q.H., Xin C.J., Xu K.S., Shu L. and Gao H.H.: Application of differential GPS to the geographic azimuth measurement in China geomagnetic field monitoring network, *China Earthquake Engineering Journal*, 37(3):863-866, DOI:10.3969/ji.ssn.1000-0844.2015.03.0862, 2015.
- 430 Lin Y, Sun J.J. and Yang X.: A review of the principles and methods of geomagnetic navigation and positioning technology, *Gnss World of China*, 48(6): 32-41, DOI: 10.12265/j.gnss.2023134, 2023.
- Liu X.J., Zhegn Y. and Li C.H.: Precise determination of astronomical azimuth by hour angle method of multiple meridian stars. *ACTA ASTRONOMICA SINICA*, 61(3):1-10, doi:10.15940/j.cnki.0001-5245.2020.03.008, 2020.
- 435 Lu Y., Wei D.Y., Ji X.C. and Yuan H.: Review of geomagnetic positioning method, *Navigation Positioning & Timing*, 9(2):118-130, doi:10.19306/j.cnki.2095-8110.2022.02.015, 2022.
- Ma H.B.: Derivation of formulas for astronomical azimuth determination and approach to the method, *Journal of Shenyang Institute of Gold Technology*, 14(3):331-336, 1995.
- Shi J.G.: Surveying data transmission method in drilling, *Petroleum Drilling Techniques*, 36(4):15-17, 2008.

- 440 State Bureau of Quality and Technical Supervision (SBQTS): Specification for the geodetic astronomy, GB/T 17943-2000, <https://openstd.samr.gov.cn> (last access: 26 May 2025), 2000.
- St-Louis, B., INTERMAGNET Operations Committee and INTERMAGNET Executive Council: INTERMAGNET Technical Reference Manual, Version 5.1.1, (INTERMAGNET), Potsdam: GFZ Data Services, 134 p. <https://doi.org/10.48440/INTERMAGNET.2024.001>, Last accessed 20 May 2025.
- 445 Solarić N. and Špoljarić D.: Accuracy of the automatic grid azimuth determination by observing the Sun using Kern E2 theodolite. *Surveying and Mapping, USA*, 48(1):19-28, 1988.
- Solarić N. and Špoljarić D.: Accuracy of the automatic astronomical azimuth determination by Polaris with Leica-Kern E2 electronic theodolite. *Surveying and Land Information System*, (2):80-85, 1992.
- Solarić N., Špoljarić D. and Nogić Č.: Analysis of the accuracy of the automatic azimuth determination by measuring zenith
- 450 distances of star with electronic theodolite Kern E2. *Hvar Obs. Bull.*, 14:1-14, 1990.
- Špoljarić D. and Solarić N.: Automation of astrogeodetic measurements. *Proceedings of the 10th International Multidisciplinary Scientific Geoconference SGEM 2010*, I:837-844, 2010.
- Šugar D., Brkić M. and Špoljarić D.: Comparison of the reference mark azimuth determination methods. *Annals of Geophysics*, 55(6):1071-1083, doi: 10.4401/ag-5405, 2012.
- 455 Torge W.: *Geodesy*. Walter de Gruyter, Berlin/New York, 2001.
- Vittuari L., Tini M. A., Sarti P., Serantoni E., Borghi A., Negusini M. and Guillaume S.: A comparative study of the applied methods for estimating deflection of the vertical in terrestrial geodetic measurements. *Sensors*, 16(4):565, doi:10.3390/s16040565, 2016.
- Wang J.B.: Discussion on GPS azimuth system conversion and its accuracy, *Beijing Surveying and Mapping*, (1): 24-27, 2001.
- 460 Wang X.Q.: The effects of multipath errors on GPS surveying, *Crustal Deformation and Earthquake*, 20(1): 56-59, 2000.
- Wang Z. Y., Jiang H. and Hou Y.J.: Azimuth angle measurement of Dalian geomagnetic station, *Azimuth angle measurement of Dalian Geomagnetic Station*, *Seismological and Geomagnetic Observation and Research*, 35(5/6):120-123, doi:10.3969/j.issn.1003-3246.2014.05/06.023.2014.
- Xu X.G., Shang X.Q. and Zhou J.P.: Measurement of astronomic azimuth angle in Jinghai station and its quality evaluation,
- 465 *Northwestern Seismological Journal*, 25(3): 281-285, 2003.
- Yang F. X., Yang X., Zhang X. Y. and Huang J. M.: Azimuth survey of Urumqi geomagnetic station marker, *Inland Earthquake*, 22(4):306-313, 2008.
- Yin W.T.: Obtaining the azimuth with GPS, *Geomatics & Spatial Information Technology*, 31(1):120-126, 2008.
- Yu J.K., Zhao R.R. and Ren Y.C.: Directional azimuth of GNSS calculation method, *Journal of Navigation and Positioning*,
- 470 6(1):120-122, doi:10.16547/j.cnki.10-1096.20180122, 2018.
- Zhang C., Zheng Y., Meng F.Y. and Chang L.L.: Measure astronomical azimuth using GPS and electronic theodolite, *Journal of Information Engineering University*, 6(2): 96-99, 2005.

- Zhang H.B., Lian Q., Kang C.K. and Zhou J.: Quantitative analysis of the relationship between geomagnetic anomaly and geological structure, *Geological and Mineral Surveying and Mapping*, 7(6): DOI:10.12238/gmsm.v7i6.1847, 2024a.
- 475 Zhang, S. Q., Fu, C. H., He, Y. F., Yang, D. M., Li, Q., Zhao, X. D., and Wang, J. J.: Quality control of observation data by the Geomagnetic Network of China, *Data Science Journal*, 15, 1–12, DOI:<http://dx.doi.org/10.5334/dsj-2016-015>, 2016.
- Zhang, S. Q., Fu, C. H., Zhao, X. D., Zhang, X. X., He, Y. F., Li, Q., Chen, J., Wang, J. J., and Zhao, Q.: Strategies in the Quality Assurance of Geomagnetic Observation Data in China, *Data Science Journal*, 23, 1–11, DOI: <https://doi.org/10.5334/dsj2024-009>, 2024b.
- 480 Zhao L.C. and Xiong Y.: Azimuth of Polaris application of new techniques to surveying astronomic, *Journal of Geomatics*, 28(3): 37-39, 2003.
- Zhou J.P., Huang W.B., Cheng A.L., et al.: Azimuth measurement and error analysis at Beijing geomagnetic observatory, *Seismological and Geomagnetic Observation and Research*, 18(6):73-79, 1997.
- Zhou Y. T., Li Y. G. and Shang Q. F.: Study on the calibration method for the difference GPS direction, *Journal of Astronautic Metrology and Measurement*, 29(4):50-53, 2009.
- 485